Catalysis Today 146 (2009) 103–109

Contents lists available at ScienceDirect

Catalysis Today

journal homepage: www.elsevier.com/locate/cattod

Sulfur-tolerant Pt/Gd_2O_3–CeO_2–Al_2O_3 catalyst for high efficiency H_2 production from autothermal reforming of retail gasoline

Qingsong Xue, Lida Gao, Yong Lu *

Shanghai Key Laboratory of Green Chemistry and Chemical Processes, Department of Chemistry, East China Normal University, North 3663 Zhongshan Road, Shanghai 200062, China

ARTICLE INFO

Article history:
Available online 14 February 2009

Keywords:
Platinum
Ceria
Gadolinia
Sulfur
Autothermal reforming
Gasoline

ABSTRACT

Pt/CeO_2–Al_2O_3 catalysts with and without Gd_2O_3 additive were prepared by stepwise incipient wetness impregnation (IWI) method. The catalysts were tested for autothermal reforming (ATR) of retail gasoline containing 158–500 ppm sulfur under the optimal reaction conditions: 800 °C, gasoline WHSV of 0.9 h^{-1} and a $H_2O/O_2/C$ molar ratio of 5/0.35/1. It is found that the content of Gd_2O_3 and impregnation procedure for catalyst preparation significantly affected the catalyst performance. Pt catalyst supported on the Al_2O_3 that was pre-impregnated with Ce and Gd nitrates orderly to 15 wt% CeO_2 and 1.6 wt% Gd_2O_3 was the best catalyst for ATR of gasoline with high reactivity and excellent stability. Within 1000-h ATR of retail gasoline over this catalyst, gasoline conversion was slowly decreased to 95% after 300-h run and then remained at ~95% throughout the test, while H_2 fraction in reformate remained at ~67% with a CH_4 fraction less than 0.6%. It is revealed that modification of Al_2O_3 with CeO_2 first and Gd_2O_3 then endowed the produced Pt catalyst with many advantageous effects such as significantly improved and stabilized Pt–CeO_2 interaction, greatly attenuated Pt-sintering, and enhanced oxygen ion conductivity of bulk CeO_2.

1. Introduction

H_2–O_2 fuel cells are the most promising alternatives for both stationary power plants and mobile power systems due to the increasing concern about environmental and pollution problems. Until widespread hydrogen refueling infrastructure exists, however, hydrogen production technology appears to be a practical option in a medium-short perspective starting from a commercial-grade high energy density liquid hydrocarbon fuels such as gasoline [1]. Gasoline fuel processing technologies have been intensively developed for both on board (especially for military and mobile uses), and off board (for stationary and residential uses) applications because of the convenient system of service station. Among the reformation technologies of gasoline, autothermal reforming (ATR) of gasoline is considered to be the preferred hydrogen production process since it has much better dynamics than a steam reforming process and permits to avoid the danger of temperature runaway [2,3].

Sulfur is well known to readily poison nickel catalysts by formation of stable surface metal sulfides and thereby prevent reactant (steam, oxygen and fuel) from adsorbing at the surface [4]. Sulfur can in principle be taken out deeply from fuels using current hydrotreating process, but quite severe operation conditions (H_2 recycling, 3–20 MPa, >300 °C) make its integration with the fuel processor dramatically difficult from both the technique and efficiency points of view. Therefore, the development of high sulfur-tolerant reforming catalyst is meaningful and practical [1]. Recently, a few special sulfur-tolerant catalysts have been mentioned in the open literature, albeit with confidential formulations [1,5,6]. A specific supported precious metal catalyst with a proprietary formulation, able to cope with 100 ppm sulfur, has been developed by Johnson Matthey for SR of higher hydrocarbons [5]. A proprietary catalyst of bimetallic compound supported on high-surface area Al_2O_3 treated with an oxide with oxygen ion-conducting properties and sulfur resistance comparable to that of the Johnson Matthey catalyst has been developed by InnovaTek [1]. The U.S. Department of Energy's Argonne National Laboratory has developed a highly sulfur-tolerant Pt/dope-ceria autothermal reforming catalyst with proprietary formulations, but only initial reaction results in the presence of sulfur have been reported [6]. Furthermore, bimetallic Rh–Ni catalysts loaded on CeO_2-modified Al_2O_3 support have been reported to be successful for SR of a JP-8 jet fuel with 22 ppm of sulfur for 72 h with >95% conversion, with Ni acting as a protective and sacrificial metal for Rh, thereby leading to much greater sulfur tolerance [7]. A novel approach that combines the concepts of shape selectivity and hydrogen spillover has been developed to design sulfur-tolerant hydrogenation catalysts; the Pt particles entrapped in the KA-zeolite cages have shown resistance to sulfur poisoning because the reduced pore opening can successfully prevent H_2S molecules from attacking Pt particles while allowing hydrogen molecules to enter freely [8]. Despite these advances, developing a reforming catalyst with significantly improved

---

* Corresponding author. Tel.: +86 21 62233424; fax: +86 21 62233424.
E-mail address: ylu@chem.ecnu.edu.cn (Y. Lu).

0920-5861/$ – see front matter © 2009 Elsevier B.V. All rights reserved.
doi:10.1016/j.cattod.2009.01.025

resistance to sulfur remains a worthwhile goal, because retail gasoline generally contains 50–300 ppm of sulfur (>300 ppm in China). In addition, the confidentiality of currently available catalyst formulations greatly restricts comprehensive research and development activities aimed at further improving the sulfur resistance of reforming catalysts for use in fuel cells.

In our previous work [9,10], we developed a promising sulfur-tolerant Pt catalyst using an aqueous solution of $H_2PtCl_6{\cdot}6H_2O$ to incipiently impregnate a fluorite-type $Ce_{0.8}Gd_{0.2}O_{1.9}$ (CGO) oxide, which possessed excellent sulfur-tolerance, high catalytic activity and significantly improved thermal stability (compared to Pt/CeO_2) in SR of *iso*-octane with 300 ppm sulfur. Nevertheless, Pt/CGO catalysts suffer from poor mechanical strength, high cost, and their structure stability is not good enough to fulfill the durability requirement.

CeO_2–Al_2O_3 oxides [11] present high thermal stability, high reducibility and good oxygen ion-conducting properties that play a key role in endowing the Pt catalysts with high sulfur resistance [12]. Our previous work showed that Pt catalysts supported on the CeO_2–Al_2O_3 oxides was able to cope with ≥300 ppm sulfur in ATR of gasoline [12] but the conversion of gasoline decreased obviously during the 100-h continuous test. Dikmen et al. [13] reported the gadolinium substituted ceria ($Ce_{1-x}Gd_xO_{2-\delta}$ ($x = 0$–0.30)) significantly enhanced the ionic conductivity and stability, which in turn can remarkably enhance the interaction at Pt and CGO interfaces thereby significantly promoting conversion of organosulfur into H_2S in the SR of *iso*-octane containing 300 ppm sulfur [9,10] with greatly improved catalyst stability. Accordingly, we anticipate to use Gd_2O_3 as promoter for achieving significant improvement of the stability of Pt/CeO_2–Al_2O_3 catalysts for ATR of retail gasoline.

In this work, we prepared a series of Gd_2O_3-doped Pt/CeO_2–Al_2O_3 catalysts and the ATR of retail gasoline containing 158–500 ppm sulfur over the as-made Pt catalysts was carried out to evaluate the feasibility. The effect of the amount of Gd_2O_3 and impregnation order of CeO_2 and Gd_2O_3 on the catalytic activity and stability of Pt/Gd_2O_3–CeO_2–Al_2O_3 catalysts was investigated. The optimal Pt catalysts demonstrated excellent sulfur-tolerance and reaction stability in 1000-h continuous test with high activity/selectivity.

2. Experimental

2.1. Catalyst preparation and characterization

First, γ-alumina (pretreated at 800 °C in static air for 2 h, 60–80 mesh, $S_{BET} = 157\ m^2/g$) supports were incipiently impregnated with cerous nitrate hexahydrate (Aldrich, 99.9%) and gadolinium nitrate hexahydrate (Aldrich, 99.9%), to obtain CeO_2–Al_2O_3, Gd_2O_3–CeO_2–Al_2O_3 (by stepwise IWI to load CeO_2 first and Gd_2O_3 then), CeO_2–Gd_2O_3–Al_2O_3 (by stepwise IWI to load Gd_2O_3 first and CeO_2 then) and (CeO_2/Gd_2O_3)–Al_2O_3 (by one-step IWI to load Gd_2O_3 and CeO_2 simultaneously). The resulting products in each steps of stepwise impregnation were dried at 110 °C overnight and calcinated at 450 °C in static air for 2 h.

Secondly, Pt active component was place onto the pore surface of the as-made CeO_2 and/or Gd_2O_3-modified Al_2O_3 supports by IWI method using $H_2PtCl_6{\cdot}6H_2O$ precursors. The wet samples were dried at 140 °C for 30 min and calcinated in static air at 600 °C for 1 h to obtain catalyst products comprising 15.0 wt% CeO_2, 0.8–4.0 wt% Gd_2O_3, 1.2 wt% Pt, Al_2O_3 balance.

The samples were characterized by H_2-temperature programmed reduction (H_2-TPR, Quantachrome ChemBET 3000 using a heating rate of 10 °C/min and a 5% H_2/Ar mixture as carrier/reductant gas at flow rate of 40 ml/min), N_2 adsorption–desorption (Quantachrome Autosorb 3B) and X-ray diffraction (XRD, Bruker D8 Advance diffractometer, using Cu Kα radiation at an acceleration voltage of 40 kV). CO-pulse chemisorption experiments were also carried out on Quantachrome ChemBET 3000 instrument to determine the Pt dispersion by assuming a CO/Pt ratio of 1.

2.2. Catalyst activity measurements

The ATR of retail gasoline was carried out with 1.0 g catalyst particulates packed into a fixed-bed continuous-flow quartz tube reactor (14 mm i.d.) and heated by a tubular furnace. The Pt catalysts were directly heated and exposed to a feed stream with no pre-reduction with hydrogen. Gasoline feed and water were controlled separately by two exact liquid pumps. Feed stream was retail gasoline with 158 ppm sulfur or that blended with thiophene to a sulfur content of 500 ppm. Two gas mass flow controllers were employed to be master of O_2 and N_2 (inner standard gas, 14 ml/min), respectively. A HP 6850 gas chromatograph equipped with a thermal conductivity detector (TCD) and a 30-m AT-plot capillary column was used to analyze H_2, N_2, CO, CO_2, and C1–C3 hydrocarbons in the effluent, using a He carrier. The column temperature was programmed from 40 °C to 160 °C at a ramp of 30 °C/min with a hold time of 3 min at each of the initial and final temperature points. Conversion was calculated by the N_2 inner standard method as described previously [9,14].

Carbon deposit was quantitatively detected by thermogravimetric analysis (TGA) on a Mettler TGA/SDTA/SF/851^e analyzer. In each trial, 50 mg of sample was used. Prior to TGA experiment, the sample was degassed by ultrapure N_2 flushing at 200 °C for 120 min at a flux rate of 60 ml/min. After that, TGA was performed in air-flow of 60 ml/min using heating rate of 10 °C/min.

3. Results and discussion

3.1. Optimizing the reaction condition and catalyst calcination temperature

The effects of reaction conditions on the ATR of gasoline were carefully investigated over the Pt/CeO_2–Al_2O_3 catalysts to obtain optimal reaction parameters. Reaction results for ATR of retail gasoline with 500 ppm sulfur using the Pt/CeO_2–Al_2O_3 catalyst vs. $H_2O/O_2/C$ molar ratio, reaction temperature and weight hourly space velocity (WHSV, to gasoline) were shown in Figs. 1–3, respectively.

As shown in Fig. 1, the gasoline conversion and the H_2 fraction were increased obviously while the concentration of CH_4 was decreased visibly with the increasing H_2O/C ratio under the specific O_2/C ratios. The conversion of gasoline was increased from 82% to about 100% as the H_2O/C ratio was increased from 2 to 5 with the O_2/C of 0.35. It is clear that the higher H_2O/C was favorable for ATR of gasoline. In addition, the use of higher O_2/C promoted the gasoline conversion and suppressed CH_4 formation, but it resulted in significant reduction of H_2 fraction in the reformate.

Fig. 2 shows that hydrogen fraction in reformate was increased from ∼59% to ∼67% as the reforming temperature was increased from 700 °C to 800 °C. In this case of increasing reaction temperature from 700 °C to 800 °C, the CH_4 fraction in reformate was decreased dramatically from about 11% to 0.4%, and meanwhile, gasoline conversion was increased sharply from ∼41% to ∼100%. As shown in Fig. 3, the gasoline conversion was decreased from ∼100% to 94%, accompanied by a lot formation of CH_4 with the increase in WHSV from 0.9 h^{-1} to 2.1 h^{-1}.

On balance, the optimal reaction conditions were identified as $H_2O/O_2/C$ molar ratio of 5/0.35/1, reaction temperature of 800 °C and WHSV of 0.9 h^{-1}.

We also examined the effects of the calcination temperature on the catalyst performance for ATR of retail gasoline. The optimal

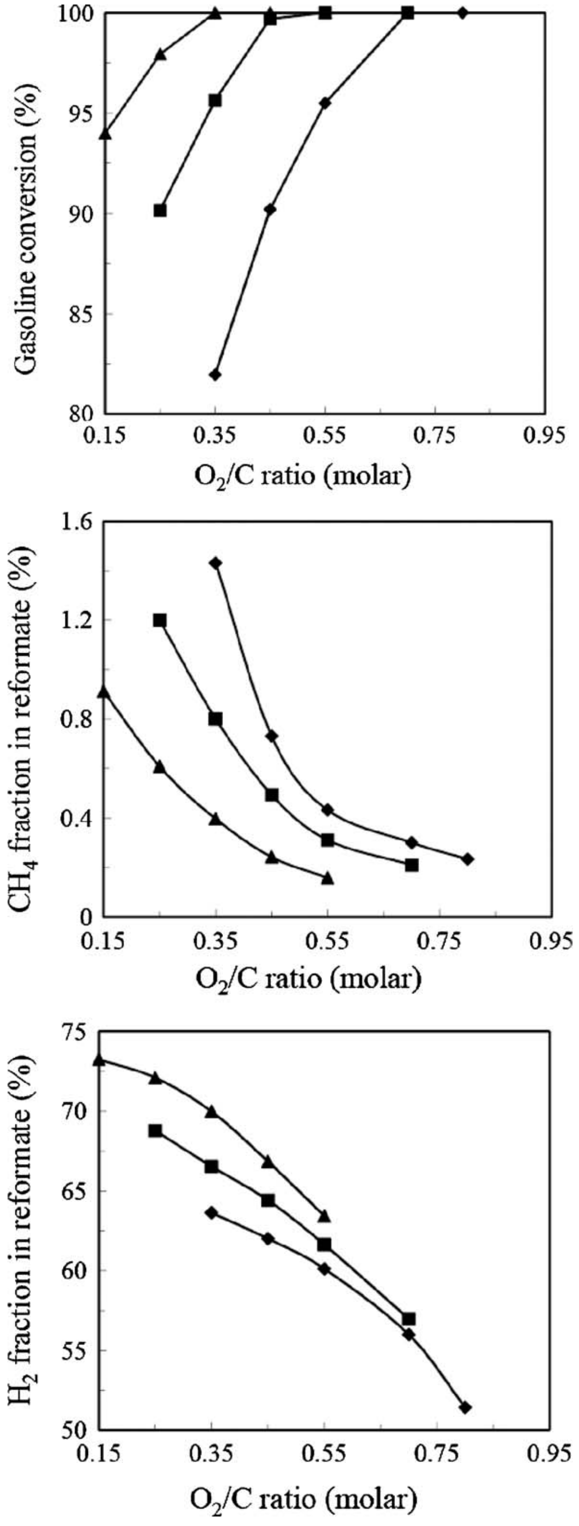

Fig. 1. Effect of $H_2O/O_2/C$ ratio on gasoline conversion and reformate composition for ATR of retail gasoline with 500 ppm sulfur over $Pt/CeO_2–Al_2O_3$ catalyst. *Note*: each reaction condition was run for 2 h during which the experimental data were collected. Reaction conditions: 800 °C, gasoline WHSV of 0.9 h^{-1}, 0.1 MPa. H_2O/C ratio of (◆) 2, (■) 3, and (▲) 5.

calcination temperature of the Gd-doped $Pt/CeO_2–Al_2O_3$ catalysts is 600 °C. Serious aggregation of both CeO_2 and Pt was observed by XRD after calcination treatment at 700 °C and 800 °C in air, and therefore their reactivity performance was significantly degraded.

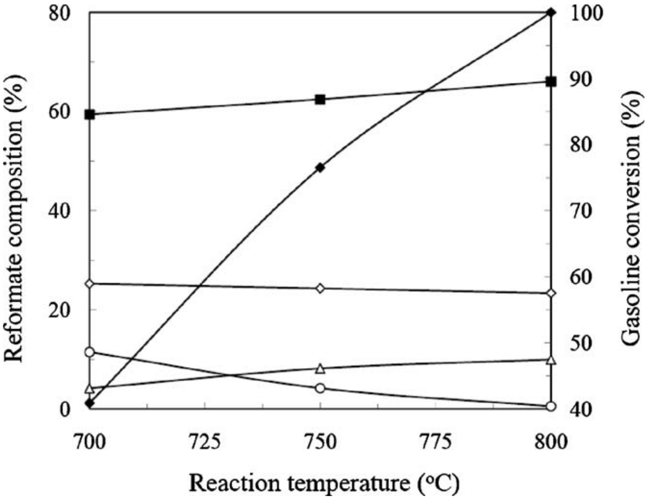

Fig. 2. Effect of reaction temperature on gasoline conversion and reformate composition for ATR of retail gasoline with 500 ppm sulfur over $Pt/CeO_2–Al_2O_3$ catalyst. *Note*: each reaction condition was run for 2 h during which the experimental data were collected. Reaction conditions: $H_2O/O_2/C$ ratio of 5:0.35:1, gasoline WHSV of 0.9 h^{-1}, 0.1 MPa. (◆) Gasoline conversion; (■) H_2; (◇) CO_2; (△) CO; (○) CH_4.

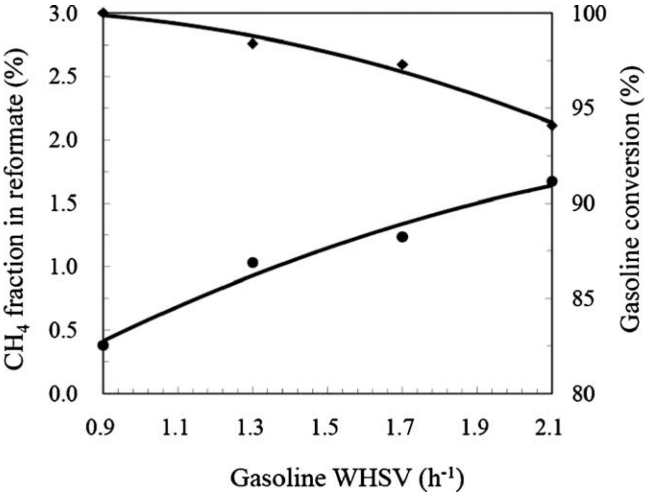

Fig. 3. Effect of gasoline WHSV on gasoline conversion and CH_4 formation for ATR of retail gasoline with 500 ppm sulfur over $Pt/CeO_2–Al_2O_3$ catalyst. *Note*: each reaction condition was run for 2 h during which the experimental data were collected. Reaction conditions: 800 °C, $H_2O/O_2/C$ ratio of 5:0.35:1, 0.1 MPa. (◆) Gasoline conversion and (●) CH_4.

3.2. Effect of Gd_2O_3 content

To gain insight into the promotive effect of Gd_2O_3 on $Pt/CeO_2–Al_2O_3$ catalysts, $Gd_2O_3–CeO_2–Al_2O_3$ with Gd_2O_3 content in range from 0.8 wt% to 4 wt% were prepared by stepwise IWI to load CeO_2 first and Gd_2O_3 then, and used to produce corresponding Pt catalysts for ATR tests and characterizations.

3.2.1. Reactivity

Fig. 4 shows the CH_4 fraction in reformate for a 50-h test for ATR of retail gasoline containing 500 ppm sulfur using $Pt/Gd_2O_3–CeO_2–Al_2O_3$ catalysts with different Gd_2O_3 contents. As we can see, CH_4 formation in the initial stage of the reaction was increased obviously with Gd_2O_3 additive content: 0.4% without Gd_2O_3 vs. 1.0% with 0.8 wt% Gd_2O_3 and up to 2.3% with 4.0 wt% Gd_2O_3. However, it should be noted that the CH_4 fraction evolution behavior was quite different with prolonged reaction time between

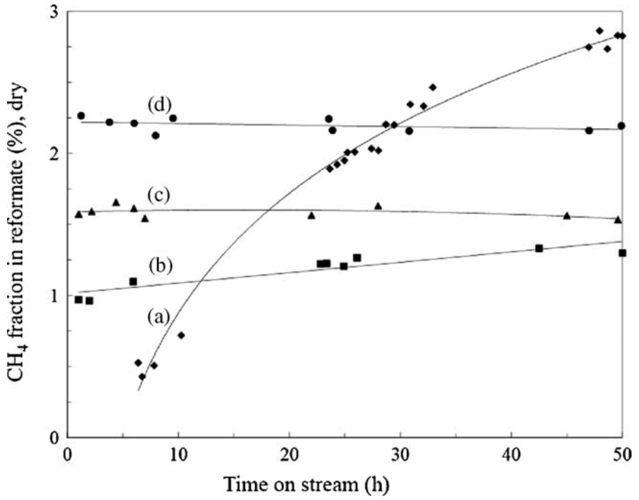

Fig. 4. CH_4 fraction in reformate product for ATR of retail gasoline with 500 ppm sulfur over (a) $Pt/CeO_2–Al_2O_3$ and $Pt/Gd_2O_3–CeO_2–Al_2O_3$ catalysts with Gd_2O_3 content of (b) 0.8 wt%, (c) 1.6 wt% and (d) 4.0 wt%, respectively. Reaction conditions: 800 °C, gasoline WHSV of 0.9 h^{-1}, $H_2O/O_2/C$ of 5/0.35/1, 0.1 MPa.

the catalysts with and without Gd_2O_3. CH_4 was formed rapidly to increase its fraction in the reformate from 0.4% to 2.8% along with the reaction time over the Pt catalyst without Gd_2O_3, due to the catalyst deactivation (gasoline conversion was decreased from ~100% to ~92% after 50-h run). In contrast, adding Gd_2O_3 additive of >0.8 wt% could sharply suppress the CH_4 formation evolution observed over the catalyst without Gd_2O_3, i.e., CH_4 fraction held the line throughout the entire 50-h run, and meanwhile, the gasoline conversion was sustained at 95–98% and the H_2 fraction remained at ~66% (not illustrated). Carefully considering methane formation and catalyst stability, we think the optimal Gd_2O_3 content should be selected around 1.6 wt%.

3.2.2. Reducibility of surface CeO_2 and interaction of Pt with CeO_2

The H_2-TPR profiles for $Pt/CeO_2–Al_2O_3$ and $Pt/Gd_2O_3–CeO_2–Al_2O_3$ catalysts are shown in Fig. 5. A main peak at ~350 °C and weak shoulder peaks at its low (~220 °C and ~300 °C) and high (~415 °C) temperature sides appeared on the $Pt/CeO_2–Al_2O_3$ catalyst (Fig. 5a). The low temperature peak is ascribable to PtO_x reduction. The main peak and shoulder peaks at ~300 °C and ~415 °C are assigned to the Pt-catalyzed reduction of surface ceria according to the literature [9,10], and such asymmetric feature is likely due to the heterogeneous properties of catalyst surface. As noted in previous work [15–19], the addition of metals can catalyze the surface reduction process, shifting the reduction peaks to lower temperature and sharpening the features but to what extent is dependent on the interaction between Pt particles and CeO_2 oxide at their interface. Moreover, a wide peak centered at ~650 °C was also observed in the H_2-TPR profile of $Pt/CeO_2–Al_2O_3$ catalyst, which is likely ascribable to the reduction of small part of bulk ceria that cannot be catalyzed by Pt-doping [20].

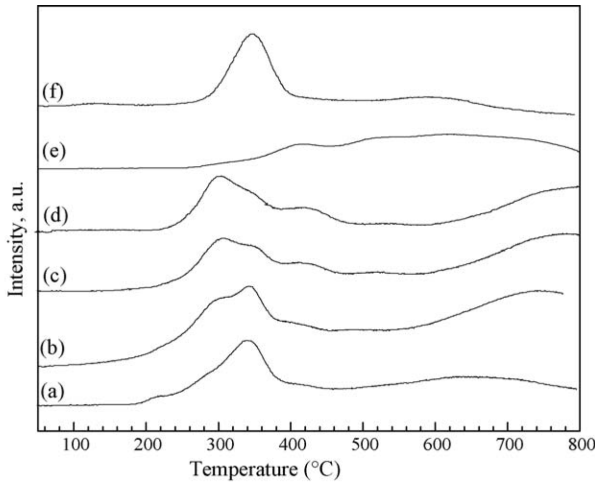

Fig. 5. H_2-TPR profiles of (a) $Pt/CeO_2–Al_2O_3$ and $Pt/Gd_2O_3–CeO_2–Al_2O_3$ catalysts with Gd_2O_3 content of (b) 0.8 wt%, (c) 1.6 wt%, (d) 4.0 wt%, (e) used sample a and (f) used sample c in Fig. 4 with 1-h treatment at 600 °C in air, respectively.

From the TPR profiles for catalysts with Gd_2O_3 additive, it is clear that the shoulder peak at ~300 °C became stronger with the increase in Gd_2O_3 content while the main peak at ~350 °C became weaker (Fig. 5b–d), suggesting that the Gd_2O_3 additive provided further enhancement of $Pt–CeO_2$ interaction thereby promoting the surface-ceria-reduction process. Dikmen et al. [13] have revealed that the oxygen vacancy concentration and the concomitant oxide ion conductivity, in cerium oxide can be increased by the substitution of a lower valent metal ion (e.g., Gd^{3+}) for CeO_2. This likely is the main cause of the promoted $Pt–CeO_2$ interaction. Our previous report has shown that such strong $Pt–CeO_2$ interaction endowed catalyst with high tolerance to sulfur poisoning [9]. The peak of PtO_x disappeared on the profiles of Fig. 5b–d, likely due to the strengthened $Pt–CeO_2$ interaction that might make PtO_x reduced at higher temperature and overlapped with the reduction of surface ceria. The peaks at ~415 °C still appeared on the profiles of Fig. 5b–d, suggesting that Gd_2O_3 additive did not facilitate the reduction of this small amount of surface CeO_2 likely because such CeO_2 species and Gd_2O_3 additives were untouchable to each other.

It also should be noted that the Gd_2O_3 additives improved the reducibility of bulk CeO_2 (i.e., enhanced oxygen ion conductivity) but did not promote this reduction process according to the observation that peak areas were increased with Gd_2O_3 additives but peak temperatures were not reduced yet. The enhanced oxygen ion conductivity of bulk CeO_2 was correlated well with the improved ability to carbon deposition resistance (see Table 1 in posterior part).

More interestingly, when we treated the used $Pt/Gd_2O_3–CeO_2–Al_2O_3$ and $Pt/CeO_2–Al_2O_3$ catalysts (those after 50-h ATR reaction in Fig. 4) at 600 °C for 1 h in air and performed H_2-TPR experiments again, it is found that a strong symmetrical peak at ~350 °C can be obtained on that catalyst with Gd_2O_3 additive (Fig. 5e) but the peak for Pt-catalyzed surface ceria became faint and shifted to higher temperature (~400 °C) on that catalyst without Gd_2O_3 additive (Fig. 5f). This observation strongly indicated that the Gd_2O_3 additive also play a key role in stabilizing the $Pt–CeO_2$ interaction thereby ensuring the maintenance of the sulfur tolerance [9] to avoid catalyst poisoning with prolonged reaction time (Fig. 4). So, it was easy to understand why $Pt/CeO_2–Al_2O_3$ was partially deactivated within a 50-h gasoline ATR test with a lot formation of CH_4 (Fig. 4) that was due to the pyrolysis of unconverted gasoline. In addition, no strong wide peak for bulk CeO_2 reduction was observed at >600 °C, because the 1-h treatment at 600 °C

Table 1
Pt dispersion and N_2-BET surface area of $Pt/Gd_2O_3–CeO_2–Al_2O_3$ catalysts with varied Gd_2O_3 content and carbon content on the used catalysts.

Gd_2O_3 content (wt%)	Pt dispersion (%)	S_{BET} (m^2/g)	Carbon deposit[a] (wt%)
0	62.4	119	3.0
0.8	55.8	115	1.9
1.6	49.2	120	1.7
4.0	41.4	114	1.5

[a] After 50-h ATR of retail gasoline with 500 ppm sulfur under reaction conditions: 800 °C, gasoline WHSV of 0.9 h^{-1}, $H_2O/O_2/C$ ratio of 5/0.35/1, 0.1 MPa.

could not allow for re-formation of bulk CeO_2. Actually, like on their used catalysts (CeO_2 phase was reduced with H_2-rich reformate during ATR at 800 °C), no bulk CeO_2 phase still was observed by XRD on those treated catalysts (same as in Fig. 5e and f).

3.2.3. Pt dispersion, N_2-BET surface area and carbon content on used catalysts

In order to reveal the nature for the observation that CH_4 was formed rapidly with the increase in the Gd_2O_3 additive, measurements on carbon content, Pt dispersion and N_2-BET surface area for the catalysts same as those employed in Fig. 4, were performed with results in Table 1. Clearly, Pt dispersion was reduced with the increase in Gd_2O_3 additive content. This is in good agreement with the tendency of initial CH_4 fraction in reformate (at the beginning of the reaction) with the increase in Gd_2O_3 additive content (Fig. 4). It is not surprising as low Pt dispersion provided definitely low gasoline conversion (e.g., 95%) under compatible reaction conditions thereby leading to the pyrolysis of unconverted gasoline into low-carbon hydrocarbons such as methane. Daniels et al. [21] reported that the Pt catalysts with La and Ce additives presented relatively low activity for high temperature dry reforming reaction due to the strong metal–support interaction (SMSI) and partial encapsulation of the metal particle. Actually, over $Pt/Gd_2O_3–CeO_2–Al_2O_3$ catalyst CH_4 fraction in reformate could be reduced visibly when the ATR reaction was operated at lower WHSV (e.g., 0.8 h^{-1}) to approach complete gasoline conversion. In addition, there is no definite correlation of CH_4 formation with the N_2-BET surface area of the catalysts.

Furthermore, carbon deposition is generally a main cause of degradation of the reforming catalysts. As shown in Table 1, the amount of carbon of those used catalysts in Fig. 4 was decreased with Gd_2O_3 content. For instance, carbon content was 1.7 wt% for the Pt catalyst with 1.6 wt% Gd_2O_3, about a half that for the one without Gd_2O_3. However, no good correlation between carbon content and CH_4 fraction in reformate after 50-h run (Fig. 4) could be obtained. Especially, for Gd_2O_3-doped catalysts carbon content and CH_4 fraction followed opposite tendency against the Gd_2O_3 content. Not surprisingly, CH_4 fraction is consistent with the observation that the conversion was decreased with the increase of Gd_2O_3 content (i.e., more the unconverted gasoline, higher the CH_4 fraction via pyrolysis process). Nevertheless, it is questioned why the carbon deposition was opposite to the reduction of conversion with the increase of Gd_2O_3 content. This is inferred that the addition of Gd_2O_3 likely facilitates the carbon elimination through the oxidation with surface CeO_2 of which the oxygen ion conductivity was promoted with the increase of addition of Gd_2O_3 [13].

3.3. Effect of Ce,Gd impregnation sequence

$CeO_2–Gd_2O_3–Al_2O_3$ (by stepwise IWI to load Gd_2O_3 first and CeO_2 then) and $(CeO_2/Gd_2O_3)–Al_2O_3$ (by one-step IWI to load Gd_2O_3 and CeO_2 simultaneously) supports were used to produce two Pt catalysts for comparison with the $Pt/Gd_2O_3–CeO_2–Al_2O_3$ catalysts (support was prepared by stepwise IWI to load CeO_2 first and Gd_2O_3 then). All of them composed 1.2 wt% Pt, 15 wt% CeO_2, 1.6 wt% Gd_2O_3, and Al_2O_3 balance.

Table 2 shows the results for 25-h ATR of retail gasoline with 158 ppm sulfur over above three catalyst samples at 800 °C. It is clear that ATR reactivity of Pt catalysts greatly depended on the impregnation sequence of Ce and Gd in support preparation stage. The catalysts showed ATR reactivity in the following order: $Pt/Gd_2O_3–CeO_2–Al_2O_3 > Pt/(CeO_2/Gd_2O_3)–Al_2O_3 \gg Pt/CeO_2–Gd_2O_3–Al_2O_3$. Within 25-h test, $Pt/(CeO_2/Gd_2O_3)–Al_2O_3$ experienced a visible activity degradation: from 99% conversion with 0.1% CH_4 fraction after 2-h run to 97% conversion with 0.3% CH_4 fraction after 25-h run. In contrast, $Pt/Gd_2O_3–CeO_2–Al_2O_3$ always offered >99% conversion and 0.1% CH_4 fraction in reformate product throughout 25-h test. $Pt/CeO_2–Gd_2O_3–Al_2O_3$ catalysts gave conversion of 74–75% with a lot of CO_2 formation. It seems that this catalyst facilitated combustion of gasoline but was not so active for the reforming reaction with H_2O and CO_2. It should be noted that $Pt/(CeO_2/Gd_2O_3)–Al_2O_3$ provided a little bit higher selectivity to H_2 than $Pt/Gd_2O_3–CeO_2–Al_2O_3$, likely due to the difference in activity for water–gas-shift reaction.

Table 2
Effect of modification of Al_2O_3 with different impregnation procedures of CeO_2 and Gd_2O_3 on the performance of produced Pt catalysts for ATR of retail gasoline with 158 ppm sulfur.

Catalyst[a]	Time on stream (h)	Conversion (%)	Product composition (%), dry			
			H_2	CO	CH_4	CO_2
$Pt/CeO_2–Gd_2O_3–Al_2O_3$	2	75	56.9	11.0	0.5	31.6
	25	74	56.9	10.5	0.9	31.8
$Pt/(CeO_2/Gd_2O_3)–Al_2O_3$	2	>99	69.8	7.1	0.1	23.0
	25	97	68.9	7.8	0.3	22.9
$Pt/Gd_2O_3–CeO_2–Al_2O_3$	2	>99	66.7	8.2	0.1	24.9
	25	>99	65.9	8.5	0.1	25.4

Reaction conditions: 800 °C, gasoline WHSV of 0.9 h^{-1}, $H_2O/O_2/C$ ratio of 5/0.35/1, 0.1 MPa.

[a] Same catalysts as used in Fig. 6.

Fig. 6 shows the H_2-TPR profiles of these three catalyst samples. $Pt/(CeO_2/Gd_2O_3)–Al_2O_3$ catalyst provided TPR evolution quite similar to $Pt/CeO_2–Al_2O_3$ (Fig. 5), indicating Gd_2O_3 additive offered no further promotive effect. However, no peak at ~300 °C that is contributed to strong $Pt–CeO_2$ interaction was detectable in TPR profile of $Pt/CeO_2–Gd_2O_3–Al_2O_3$ catalyst, indicating that Gd_2O_3 additive produced negative effect in this case thereby leading to significant degradation of ATR of gasoline (Table 2).

3.4. Longer term test of Gd_2O_3-doped $Pt/CeO_2–Al_2O_3$ catalysts

Longer term tests for ATR of retail gasoline with 158 ppm sulfur were then performed over $Pt/(CeO_2/Gd_2O_3)–Al_2O_3$ and $Pt/Gd_2O_3–CeO_2–Al_2O_3$ catalysts with the results as displayed in Figs. 7 and 8, respectively. As expected, the $Pt/(CeO_2/Gd_2O_3)–Al_2O_3$ catalyst was

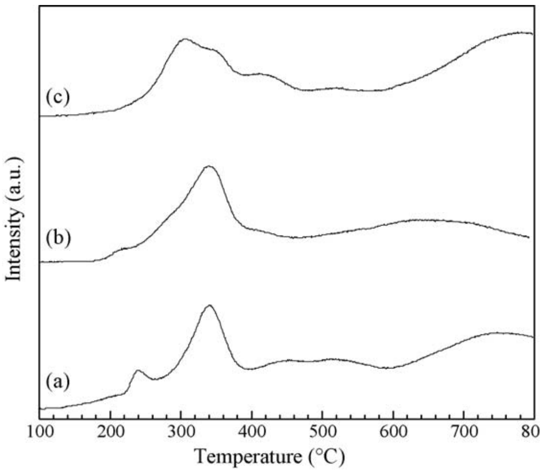

Fig. 6. H_2-TPR profiles of (a) $Pt/CeO_2–Gd_2O_3–Al_2O_3$, (b) $Pt/(CeO_2/Gd_2O_3)–Al_2O_3$ and (c) $Pt/Gd_2O_3–CeO_2–Al_2O_3$ catalysts, where supports were prepared by: for sample a, stepwise IWI to load Gd_2O_3 first and CeO_2 then; for sample b, one-step impregnation to load CeO_2 and Gd_2O_3 simultaneously; for sample c, stepwise IWI to load CeO_2 first and Gd_2O_3 then. *Note*: all these three samples had same composition: 1.2 wt% Pt, 15 wt% CeO_2, 1.6 wt% Gd_2O_3, and Al_2O_3 balance.

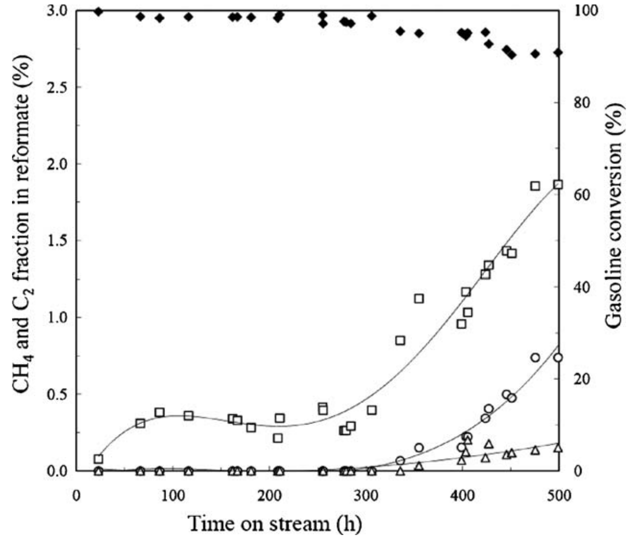

Fig. 7. Longer term for ATR of retail gasoline with 158 ppm sulfur over Pt/(CeO_2/Gd_2O_3)–Al_2O_3 catalyst of which the support was prepared by one-step impregnation to load CeO_2 and Gd_2O_3 simultaneously. Reaction conditions: 800 °C, gasoline WHSV of 0.9 h^{-1}, $H_2O/O_2/C$ ratio of 5/0.35/1, 0.1 MPa. (◆) Gasoline conversion, (□) CH_4, (○) C_2H_4, and (△) C_2H_6.

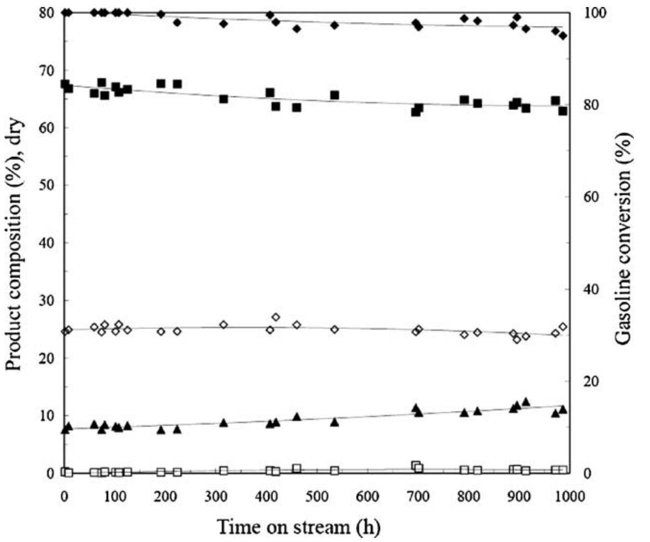

Fig. 8. Longer term for ATR of retail gasoline with 158 ppm sulfur over Pt/Gd_2O_3–CeO_2–Al_2O_3 catalyst of which the support was prepared by stepwise IWI to load CeO_2 first and Gd_2O_3 then. Reaction conditions: 800 °C, gasoline WHSV of 0.9 h^{-1}, $H_2O/O_2/C$ ratio of 5/0.35/1, 0.1 MPa. (◆) Gasoline conversion, (■) H_2, (◇) CO_2, (▲) CO and (□) CH_4.

not so good to ensure the maintenance of the activity within a longer term run. The main cause lies in that the Gd_2O_3 additive did not work to further strengthen Pt–CeO_2 interaction for this catalyst (see Fig. 6). As shown in Fig. 7, gasoline conversion was decreased to ~97% after 25 h and remained at ~97% until to 300 h, but then was decreased again slowly to ~91% during another 200 h. Within first 300-h run, CH_4 in the reformate was increased slowly from 0.1% to 0.4% and no C2 hydrocarbons were formed. After 300-h run, however, CH_4 and C2 hydrocarbons were formed rapidly and reached to 1.9% and 0.9% after run for 500 h. Carbon content of this used catalyst was determined to be 13 wt%.

In contrast, Pt/Gd_2O_3–CeO_2–Al_2O_3 catalyst showed excellent reaction stability. It is not surprising as modification of Al_2O_3 by stepwise IWI method to load CeO_2 first and Gd_2O_3 then resulted in significant improvement of Pt–CeO_2 interaction (Fig. 5). As shown in Fig. 8, gasoline conversion was slowly decreased from >99% to 95–97% within 300 h and then was sustained at >95% within another 700 h. H_2 fraction in reformate remained at ~67% while CH_4 in reformate was retained at <0.6% throughout the entire 1000-h test. Moreover, no any C2 products were formed in this course. Carbon content of this used catalyst was determined to be <5 wt% (less than a half that for Pt/(CeO_2/Gd_2O_3)–Al_2O_3 after 500-h run), likely due to promoted high temperature oxygen ion conductivity. Furthermore, only a very weak Pt(1 1 1) XRD peak at 2θ of 39.8° was detectable on the used Pt/Gd_2O_3–CeO_2–Al_2O_3 catalyst; but a quite strong Pt(1 1 1) peak appeared on the used Pt/(CeO_2/Gd_2O_3)–Al_2O_3 catalyst, even though it experienced only 500-h run (a half that for Pt/Gd_2O_3–CeO_2–Al_2O_3 catalyst). The above XRD results indicated that strong and stable Pt–CeO_2 interaction also greatly suppressed the sintering of Pt, being consistent with the observation in previous work [9,22,23].

4. Conclusions

A promising Gd_2O_3-doped Pt/CeO_2–Al_2O_3 catalyst has been developed for ATR of retail gasoline with 158 ppm sulfur or more. It is found that the catalyst performance is strongly dependent on the catalyst preparation procedure. Modification of Al_2O_3 by stepwise IWI method with CeO_2 first and Gd_2O_3 then, followed by placing Pt onto as-made support, has proven to be the most effective and efficient way for obtaining a high-performance ATR catalyst. By doing so, Gd_2O_3 additive provides advantageous effects such as significant improvement and stabilization of Pt–CeO_2 interaction, great attenuation of Pt-sintering and enhancement of oxygen ion conductivity of bulk CeO_2. As a result, the resulting catalyst maintains its activity and selectivity, with low level of carbon deposition, throughout 1000-h ATR of retail gasoline containing 158 ppm sulfur at 800 °C and WHSV (gasoline) of 0.9 h^{-1} with $H_2O/O_2/C$ molar ratio of 5/0.35/1. In addition, Gd_2O_3 additive also delivers significant promotion on the carbon resistance of the catalysts.

Acknowledgments

Lu gratefully thanks the Program for New Century Excellent Talents in University (NCET-06-0423), Shuguang Project (06SG28) and Shanghai Leading Academic Discipline Project (B409). This work is supported by grants from the National Natural Science Foundation of China (20590366 and 20573036), the Ministry of Science and Technology of China (2007AA05Z101), and the PhD Program Scholarship Fund of ECNU 2008 (20080013).

References

[1] Q. Ming, T. Healey, L. Allen, P. Irving, Catal. Today 77 (2002) 51.
[2] D.L. Trimm, Z.I. Onsan, Catal. Rev. 43 (2001) 31.
[3] C.S. Song, Catal. Today 77 (2002) 17.
[4] D.J. Moon, J.W. Ryu, S.D. Lee, B.G. Lee, G. Byung, B.S. Ahn, Appl. Catal. A 272 (2004) 53.
[5] A.F. Ghenciu, Curr. Opin. Solid State Mater. Sci. 6 (2002) 389.
[6] M. Krumpelt, T.R. Krause, J.D. Carter, J.P. Kopasz, S. Ahmed, Catal. Today 77 (2002) 3.
[7] J.J. Strohm, J. Zheng, C.S. Song, J. Catal. 238 (2006) 309.
[8] H. Yang, H.L. Che, J.W. Chen, O. Omotoso, Z. Ring, J. Catal. 243 (2006) 36.
[9] Y. Lu, J. Chen, Y. Liu, Q. Xue, M. He, J. Catal. 254 (2008) 39.
[10] Y. Lu, J. Chen, Q. Xue, Y. Liu, M. He, Stud. Surf. Sci. Catal. 172 (2007) 273.
[11] S. Damyanova, C.A. Perez, M. Schmal, J.M.C. Bueno, Appl. Catal. A 234 (2002) 271.
[12] Y. Lu, Q. Xue, L. Gao, P. Zhu, Y. Liu, M. He, Chinese Patent, CN: 101143320A (2007).
[13] S. Dikmen, P. Shuk, M. Greenblatt, H. Gocmez, Solid State Sci. 4 (2002) 585.
[14] L. Wang, K. Murata, M. Inaba, Appl. Catal. A 257 (2004) 43.
[15] T. Shido, Y. Iwasawa, J. Catal. 136 (1992) 493.
[16] G. Jacobs, E. Chenu, P.M. Patterson, L. Williams, D. Sparks, G. Thomas, B.H. Davis, Appl. Catal. A 258 (2004) 203.
[17] G. Jacobs, P.M. Patterson, L. Williams, E. Chenu, D. Sparks, G. Thomas, B.H. Davis, Appl. Catal. A 262 (2004) 177.
[18] H.C. Cao, Y.F.Y. Yao, J. Catal. 86 (1984) 254.

[19] G. Jacobs, U.M. Graham, E. Chemu, P.M. Patterson, A. Dozier, B.H. Davis, J. Catal. 229 (2005) 499.
[20] S. Damyanova, J.M.C. Bueno, Appl. Catal. A 253 (2003) 135.
[21] J.J. Daniels, R.A. Arther, L.B. Lee, S.M. Stagg-Williams, Catal. Lett. 103 (2005) 169.
[22] Y. Nagai, T. Hirabayashi, K. Dohmae, N. Takagi, T. Minami, H. Shinjoh, S. Matsumoto, J. Catal. 242 (2006) 103.
[23] S. Bernal, J.J. Calvino, M.A. Cauqui, J.M. Gatica, C. Larese, J.A. Perez Omil, J.M. Pintado, Catal. Today 50 (1999) 175.